Report

Neuron

Dynein Regulator NDEL1 Controls Polarized Cargo Transport at the Axon Initial Segment

Highlights

- NDEL1 redistributes from the centrosome to the AIS during neurodevelopment
- Dynein regulator NDEL1 stably binds to Ankyrin-G at the AIS
- The motor protein dynein drives transport of somatodendritic cargo out of the AIS
- Accumulation of NDEL1 at the AIS is necessary for efficient local cargo reversal

Authors

Marijn Kuijpers, Dieudonnée van de Willige, Amélie Freal, ..., Anna Akhmanova, Dick Jaarsma, Casper C. Hoogenraad

Correspondence

c.hoogenraad@uu.nl

In Brief

Polarized cargo transport ensures the sorting of vesicles specifically into the axon or dendrites. Kuijpers et al. reveal a critical role for dynein regulator NDEL1 as a gatekeeper of somatodendritic cargos at the axon initial segment.

Kuijpers et al., 2016, Neuron *89*, 461–471
February 3, 2016
http://dx.doi.org/10.1016/j.neuron.2016.01.022

CellPress

Neuron
Report

Dynein Regulator NDEL1 Controls Polarized Cargo Transport at the Axon Initial Segment

Marijn Kuijpers,[1,3] Dieudonnée van de Willige,[1,3] Amélie Freal,[1] Anaël Chazeau,[1] Mariella A. Franker,[1] Jasper Hofenk,[1] Ricardo J. Cordeiro Rodrigues,[1] Lukas C. Kapitein,[1] Anna Akhmanova,[1] Dick Jaarsma,[2] and Casper C. Hoogenraad[1,*]
[1]Cell Biology, Department of Biology, Faculty of Science, Utrecht University, 3584 CH Utrecht, the Netherlands
[2]Department of Neuroscience, Erasmus Medical Center, 3015 CE Rotterdam, the Netherlands
[3]Co-first author
*Correspondence: c.hoogenraad@uu.nl
http://dx.doi.org/10.1016/j.neuron.2016.01.022

SUMMARY

The development and homeostasis of neurons relies heavily on the selective targeting of vesicles into axon and dendrites. Microtubule-based motor proteins play an important role in polarized transport; however, the sorting mechanism to exclude dendritic cargo from the axon is unclear. We show that the dynein regulator NDEL1 controls somatodendritic cargo transport at the axon initial segment (AIS). NDEL1 localizes to the AIS via an interaction with the scaffold protein Ankyrin-G. Depletion of NDEL1 or its binding partner LIS1 results in both cell-wide and local defects, including the non-polarized trafficking of dendritic cargo through the AIS. We propose a model in which LIS1 is a critical mediator of local NDEL1-based dynein activation at the AIS. By localizing to the AIS, NDEL1 facilitates the reversal of somatodendritic cargos in the proximal axon.

INTRODUCTION

Due to their distinct functions, axons and dendrites differ in their molecular organization and require specific building blocks and cellular materials. The axon initial segment (AIS) is a specialized compartment in the proximal axon that plays a critical role in separating the somatodendritic and axonal compartments, and in maintaining the molecular and functional polarity of the neuron (Rasband, 2010). The AIS forms a diffusion barrier for membrane proteins at the cell surface and regulates selective intracellular cargo traffic between the soma and the axon (Leterrier and Dargent, 2014). Vesicles containing somatodendritic cargo enter the axon but very rarely move beyond the AIS, whereas cargoes transporting axonal proteins proceed through the AIS into more distal parts (Al-Bassam et al., 2012; Petersen et al., 2014). However, the molecular processes that control selective transport at the AIS remain unclear.

There is strong evidence that cytoskeleton-based motor proteins drive selective transport to sort cargo into axons and dendrites. One model suggests that filamentous actin at the AIS may contribute to selective transport by halting somatodendritic vesicles and serving as a substrate for myosin-mediated vesicle transport (Lewis et al., 2009; Watanabe et al., 2012). Another model proposes that targeting of polarized cargo is determined by a distinct microtubule (MT) organization between axons and dendrites, in combination with the coordinated regulation of MT-based motor proteins (Kapitein and Hoogenraad, 2011). In this way, the unidirectional axonal MT organization facilitates plus-end-directed kinesin movements, resulting in axonal targeting (Kapitein et al., 2010; Nakata and Hirokawa, 2003). In contrast, MT minus-end-directed dynein drives retrograde axonal transport. Its function as key retrograde axonal motor raises the question whether dynein also plays a role in preventing somatodendritic cargo from entering the axon. However, whether dynein-mediated somatodendritic vesicle sorting plays a role at the AIS is unexplored.

In this study, we demonstrate that dynein and its regulator Nuclear distribution element-like 1 (NDEL1) control cargo sorting at the AIS. Our data show that NDEL1 is concentrated at the AIS via interaction with the AIS scaffold protein Ankyrin-G (AnkG) and that depletion of NDEL1 or its binding partner LIS1 leads to the entry of dendritic cargo into the proximal axon. We propose a model in which LIS1 is a critical mediator of NDEL1-based dynein activation at the AIS, and in which AIS-bound NDEL1 facilitates the local direction reversal of somatodendritic vesicles. These results suggest a new mechanism for selective vesicle filtering at the AIS and reveal a critical role for NDEL1 as a gatekeeper of somatodendritic transport cargos.

RESULTS

Dynein Regulators NDEL1 and LIS1 Localize to the AIS

To determine whether dynein plays a role in somatodendritic cargo transport at the AIS, we screened the subcellular distribution of dynein components, dynactin, and other dynein regulators in developing and mature neurons. Most dynein and dynactin antibodies showed diffuse cytoplasmic staining throughout the axon shaft, with a higher intensity in the growth cones (Figure S1 and data not shown). The NDEL1 antibody we used in this study is specific for NDEL1, as it did not recognize the NDEL1 homolog NDE1 (Figure 1A). Consistent with previous studies (Niethammer et al., 2000; Sasaki et al., 2000), NDEL1 expression increased as neurons developed (Figure 1B). Immunocytochemistry of neurons at DIV1 showed

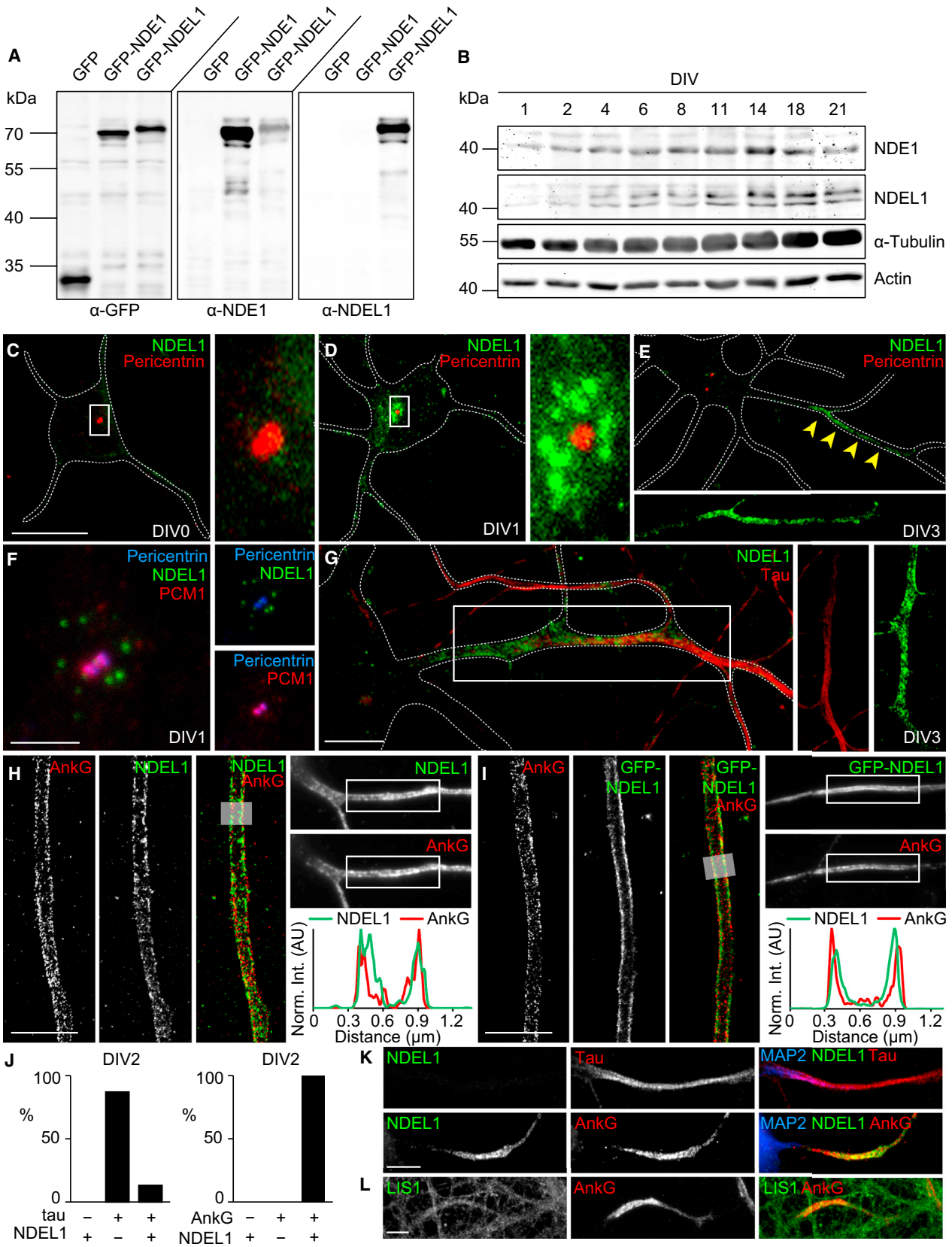

(legend on next page)

that NDEL1 was predominantly present around the centrosome as labeled by pericentrin and the pericentriolar marker PCM1 (Figures 1C, 1D, 1F, and S1A). We found that NDEL1 staining was lost from the pericentriolar region at later stages of neuronal development (Figure 1E). Remarkably, however, in day in vitro 3 (DIV3) neurons NDEL1 showed a preferential localization in the proximal part of the axon (Figure 1G). Furthermore, the axonal NDEL1 staining pattern overlapped with AnkG staining, which outlines the AIS (Figure S2A). Super-resolved images also indicated a strong degree of co-localization of both endogenous and overexpressed NDEL1 with AnkG at the AIS membrane (Figures 1H and 1I). To analyze the redistribution of NDEL1 during axogenesis and AIS formation, stage 3 neurons were fixed at DIV2 and stained for tau, AnkG, and NDEL1. At this stage, only 10% of tau-positive axons were positive for NDEL1, indicating that NDEL1 distribution to the AIS occurred after axon specification. In contrast, AIS localization of NDEL1 was observed in 100% of AnkG-positive axons (Figures 1J and 1K), suggesting that AnkG and NDEL1 localize to the AIS around the same time. Interestingly, LIS1, a binding partner of NDEL1 (Niethammer et al., 2000; Sasaki et al., 2000), is expressed throughout the neuron and is enriched at the growth cone but also showed a preferential localization in the proximal part of the axon in ~60% of neurons (Figures 1L, S1B, and S1C).

The homolog of NDEL1, NDE1, is predominantly present at early embryogenesis in proliferating neuronal progenitors and migrating neurons (Feng et al., 2000). We could detect endogenous NDE1 expression in cortical neuron extracts, but no specific staining was found at the AIS or elsewhere in hippocampal neurons (Figure 1B and data not shown). However, low-level expression of GFP-tagged NDE1 yielded AIS localization (Figure S2C), suggesting that exogenous NDE1 interacts with the AIS. However, whether this interaction is physiologically relevant remains unclear. Finally, to determine whether NDEL1 localized at the AIS of neurons of the adult central nervous system (CNS), we performed immunohistochemistry of NDEL1 and AnkG on brain sections of adult mice. NDEL1 co-distributed with AnkG throughout the CNS and is present at the AIS of all neuronal types examined (Figures S2D–S2H). Together, these data indicate that NDEL1 shifts its localization from a pericentriolar region to the AIS during neuron differentiation. Consistent with previous immunohistochemistry data, both NDEL1 and LIS1 are present at the AIS in more mature neurons (Sasaki et al., 2000).

NDEL1 Interacts with the Neuron-Specific Isoform of AnkG

To better understand the role of NDEL1 and LIS1 at the AIS, we searched for binding partners by performing pull-down assays combined with mass spectrometry. Bio-GFP-LIS1, -NDE1, and -NDEL1 bound to several components of dynein and dynactin (Figure 2A), confirming the previously identified interactions with the dynein complex (Niethammer et al., 2000; Sasaki et al., 2000). In addition, we identified novel potential NDEL1 binding partners, including α-actinin, AnkG, βIV-spectrin, and synaptopodin. These proteins were all described to be abundantly present at the AIS (Sánchez-Ponce et al., 2012). We also found these proteins highly enriched in the NDE1 but not in the LIS1 pull-down fraction (Figure 2A). Mass spectrometry results were confirmed by western blotting and GFP pull-down experiments (Figures 2D and 2E), demonstrating that both NDE1 and NDEL1 associate with components of the AIS.

AnkG is essential for AIS assembly and required for clustering of most other AIS components (Rasband, 2010). The two largest AnkG isoforms, AnkG-270 and AnkG-480, are neuron specific and contain serine-rich and tail domains that contribute to restriction of AnkG at the AIS (Zhang and Bennett, 1998). To identify the region through which AnkG interacts with NDEL1, we made truncated AnkG-270-GFP constructs encoding either the serine-rich and tail domains or an AnkG variant lacking these domains (Figure 2B). Pull-down experiments showed that NDEL1 only co-precipitates with AnkG fragments that contain the neuron-specific serine-rich and tail domains (Figure 2F). We next generated several NDEL1 truncations, including the N-terminal domain (NDEL1-N) that binds to dynein and LIS1 (Segal et al., 2012), and the C-terminal domain (NDEL1-C) (Figure 2C). AnkG only co-precipitated with GFP-NDEL1 constructs that contained the C-terminal fragment (Figure 2G). When expressed in neurons, the NDEL1 N terminus showed a diffuse expression pattern throughout the neuron, while the NDEL1 C-terminal domain localized to the AIS (Figure 2H). Together, these data show that the C terminus of NDEL1 interacts with the neuron-specific isoform of AnkG.

AnkG Is Required for AIS Localization of NDEL1

To determine the turnover of NDEL1 at the AIS, we performed fluorescence recovery after photobleaching (FRAP) analysis of GFP-NDEL1 compared to GFP-AnkG and GFP-tau in axons of DIV11 neurons (Figure 2I). GFP-tau fluorescence recovered rapidly in axons and reached a maximal recovery of ~95% within

Figure 1. NDEL1 Shifts from a Pericentriolar to an Axon Initial Segment Localization

(A) Lysates of HEK293 cells transfected with indicated constructs and probed on immunoblot.

(B) Western blot of DIV1–DIV21 cortical neuron lysates probed by the indicated antibodies.

(C–E) Cultured hippocampal neurons stained for pericentrin (red) and NDEL1 (green).

(F) DIV1 neuron stained for pericentrin (blue), NDEL1 (green), and PCM1 (red).

(G) DIV3 neuron stained for NDEL1 (green) and axonal marker tau (red).

(H and I) dSTORM images and line scans of DIV5 neurons, stained for AnkG (red) and NDEL1 (green) (H) or GFP-NDEL1 (green) (I). Left: dSTORM reconstructions; top right: widefield images (white boxes indicate super-resolved area); bottom right: line scans of fluorescence intensity along the transparent white line indicated in the dSTORM reconstruction image.

(J) Percentage of axons positive for NDEL1 and tau (left) or AnkG (right) at DIV2. n = 50–100 cells.

(K) Axons of DIV1 neurons stained for MAP2 (blue), NDEL1 (green), and tau or AnkG (red).

(L) DIV11 neuron with LIS1 enrichment (green) at the AIS (marked by AnkG, red).

Scale bars represent 20 μm in (C), 3 μm in (F), (H), and (I), and 5 μm in (G), (K), and (L).

A

protein	accession	Unique peptides LIS1	NDE1	NDEL1
Lissencephaly 1 (LIS1)	P63004	**28**	25	23
nuclear distribution gene E homolog 1 (NDE1)*	Q9NXR1	20	**24**	14
nuclear distribution gene E-like homolog 1 (NDEL1)	Q78PB6	13	6	**22**
Dynein 1 heavy chain (HC)	P38650	79	175	176
Dynein 1 intermediate chain 1 (IC1)	G3V792	0	13	17
Dynein 1 intermediate chain 2 (IC2)	Q62871	4	11	13
Dynein 1 light intermediate chain 1 (LIC1)	G3V7G0	0	13	17
Dynein 1 light intermediate chain 2 (LIC2)	Q62698	4	12	13
Dynein Roadblock light chain 1 (LRB1)	P62628	0	2	3
Dynein LC8 light chain 1 (LL1)	P63170	0	2	2
Dynein LC8 light chain 2 (LL2)	Q78P75	0	3	2
Dynactin 1 (p150)	D4A8U7	0	5	3
Dynactin 2 (p50 dynamitin)	Q6AYH5	0	4	0
F-actin-capping protein subunit beta	Q5XI32	2	9	8
Actinin, Alpha 2	D3ZCV0	6	33	35
Beta-IV Spectrin	F1LSL8	0	18	20
AnkyrinG	F1LNM3	0	17	15
Synaptopodin	Q9Z327	0	13	8

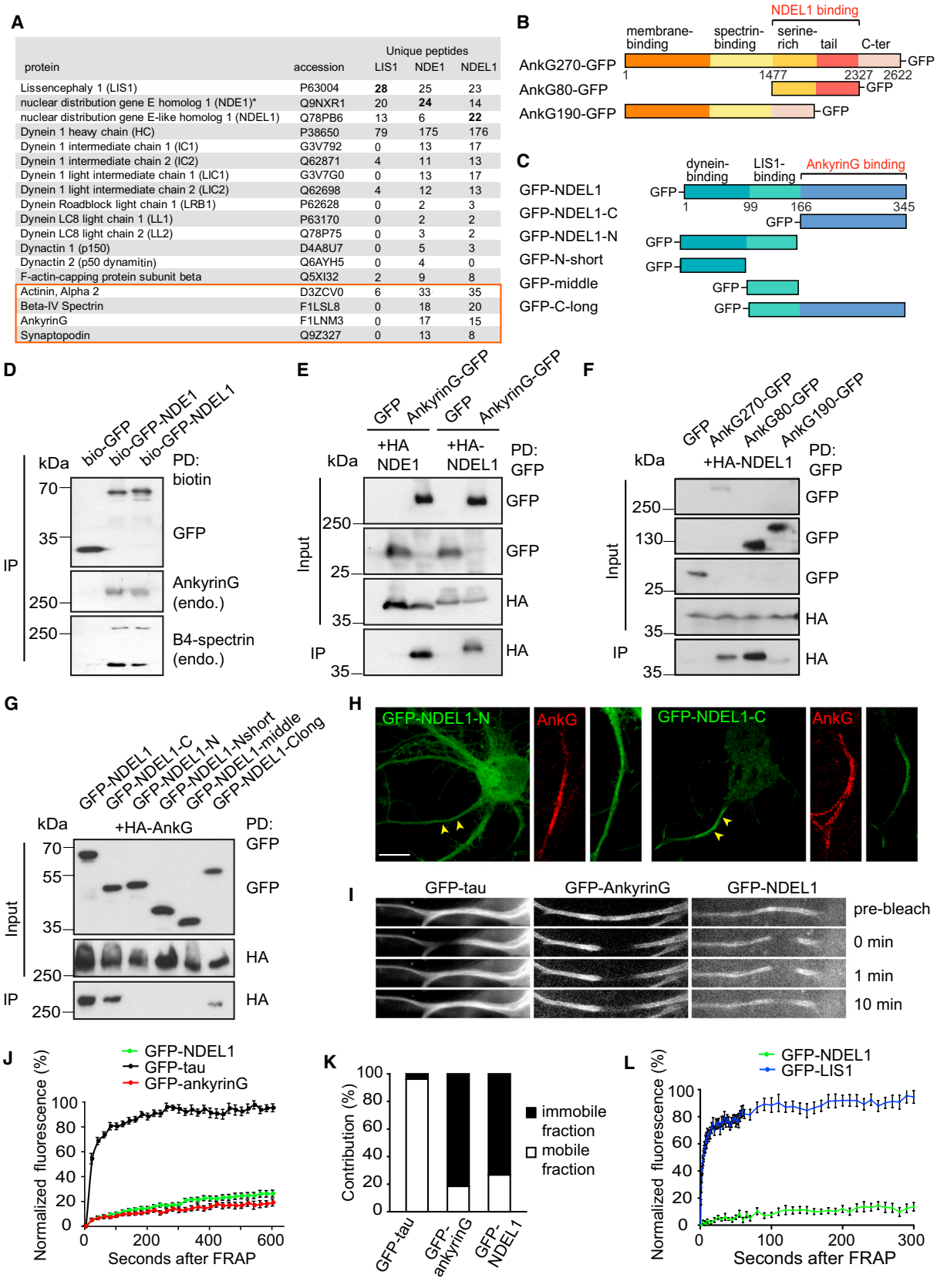

(legend on next page)

10 min. However, GFP-NDEL1 fluorescence had a much slower recovery reaching a maximum of ~20%–25% and behaved similar to that of GFP-AnkG (Figure 2J), indicating that at the AIS a large fraction of NDEL1 molecules is immobile (Figures 2J and 2K). In contrast, FRAP analysis of GFP-LIS1 showed fast recovery at the AIS, suggesting that LIS1 is not stably bound to the AIS (Figure 2L). NDEL1 staining disappeared from the AIS after knockdown of AnkG (Figures S3C–S3E) and was slightly reduced in LIS1-depleted cells (Figures S3A and S3B), indicating that recruitment of NDEL1 to the AIS depends on AnkG and to some extent on LIS1. Upon drug-induced disruption of the MT or actin cytoskeleton, both AnkG and NDEL1 were still present at the AIS, suggesting that their localization is not largely dependent on the underlying cytoskeleton (Figures S3F and S3G). Taken together, these data show that both AnkG and NDEL1 are stably present at the AIS and that AnkG and LIS1 are required for the AIS localization of NDEL1.

To test the role of NDEL1 at the AIS, we generated two independent shRNAs against NDEL1 (Raaijmakers et al., 2013; Shu et al., 2004) and performed knockdown experiments in hippocampal neurons. Efficiency of shRNA knockdown was verified by immunostaining of endogenous NDEL1 (Figures 3A and 3B). In addition, we used the CRISPR/Cas9 system (Incontro et al., 2014) to silence NDEL1 expression in hippocampal neurons (Figures S4A and S4C). In contrast to the loss of NDEL1 staining after AnkG knockdown (Figures S3C and S3E), NDEL1 knockdown or silencing did not affect the levels of AnkG at the AIS (Figures 3B and S4B). We next determined whether NDEL1 influences the localization of other dynein/dynactin components at the AIS. Both NDEL1 overexpression and depletion did not affect the diffuse cytoplasmic staining of the light intermediate chain of dynein, the p150 subunit of dynactin, or LIS1 at the AIS (Figures S3H and S3I). In addition, inhibition of the dynein/dynactin complex by overexpressing GFP-p150-cc1 did not affect NDEL1 localization (Figure S3J). These data suggest that NDEL1 is not required for AIS integrity or dynein/dynactin localization in the proximal axon and that its AIS localization does not depend on dynein/dynactin activity.

NDEL1 Depletion Causes Axonal Enlargement

Homozygous NDEL1 knockout mice die at early embryonic stages, while brain-specific mutants show severe cortical neuronal migration defects (Sasaki et al., 2005; Shu et al., 2004; Youn et al., 2009). Analyses of mature neurons in conditional NDEL1 knockout mice revealed defects in axon and dendrite morphology and aberrant axonal enlargement at the AIS (Hippenmeyer et al., 2010). We analyzed the morphological defects in cultured neurons. Consistent with the in vivo data, NDEL1 depletion caused a decrease in axonal and dendritic length (Figures 3D–3F) and resulted in increased axonal diameter both at the AIS (Figures 3G, S4A, and S4D) and more distally (Figures 3H and S4D). We further analyzed the axonal enlargement and found that shRNA-mediated depletion of LIS1 (Figures 3A and 3C) or expression of dominant-negative dynactin (p150-cc1) also increased AIS thickness (Figures S5A and S5B), suggesting that regulation of dynein activity is required for normal axon morphology. The axonal phenotype of NDEL1 depletion was rescued by co-expressing full-length NDEL1 (Figures S5C and S5D). In contrast, NDEL1 N- and C-terminal fragments were not able to restore normal axon diameter (Figures S5C and S5D). Instead, NDE1 co-expression reduced axonal enlargement of NDEL1-depleted neurons, compatible with functional redundancy between NDE1 and NDEL1 (Figure S5E). LIS1 overexpression did not attenuate axonal enlargement in NDEL1-depleted neurons, suggesting that NDEL1 is required for LIS1 function in maintaining axon caliber (Figure S5E). Similarly, axonal enlargement induced by LIS1 depletion could not be rescued by NDEL1 or NDE1 (Figure S5F). Finally, we determined the axon diameter of AnkG-depleted neurons, where NDEL1 is still present yet no longer concentrated at the AIS. As reported previously (Hedstrom et al., 2008; Sobotzik et al., 2009), axons of AnkG knockdown neurons only showed a mild and local increase of axon diameter due to dendrite-like characteristics of the proximal axon (Figure 3H), which did not resemble the morphology of axons of NDEL1-depleted neurons (Figure S5K). Using a complimentary approach, we overexpressed the NDEL1 C terminus to displace endogenous NDEL1 from the AIS and found no differences in axon caliber (Figure S5I). In conclusion, NDEL1 is required for maintenance of axon caliber, but this function is most likely independent of its accumulation at the AIS.

Altered Cytoskeleton Organization in NDEL1-Depleted Axons

What mechanisms could explain the axonal enlargement in NDEL1-depleted neurons? We examined the effect of NDEL1 knockdown on axonal MT dynamics and organization, neurofilaments, and actin. Consistent with previous data (Nguyen et al., 2004), neurofilament content was reduced when NDEL1 was depleted or dynein function was inhibited (Figure S6A). F-actin appeared unaffected in the proximal axon (Figures S6B and S6C), although periodic ring-like structures were disrupted (Figure S6D). While NDEL1-depleted neurons did not differ from

Figure 2. NDEL1 Stably Localizes to the AIS by Binding to AnkG

(A) Binding partners of bio-GFP-LIS1, -NDE1, and -NDEL1 from rat brain extracts identified by mass spectrometry. For proteins marked with *, only human peptides were identified.

(B and C) Overview of AnkG (B) and NDEL1 (C) truncations.

(D and E) Western blot analysis of biotin (D) and GFP (E) pull-downs from extracts of HEK293 transfected with the indicated constructs, probed for GFP and endogenous AnkG and βIV-spectrin (D) or GFP and HA (E).

(F and G) Binding domain analysis with GFP-AnkG truncations and HA-NDEL1 (F) or with GFP-NDEL1 truncations and HA-AnkG (G).

(H) Neurons transfected with GFP-tagged NDEL1 N or C terminus and stained for AnkG (red). Scale bar represents 10 μm.

(I) GFP-tau, -AnkG, or -NDEL1 recovery after photobleaching at the AIS of DIV7 neurons.

(J) Quantification of GFP fluorescence recovery in photobleached axons as in (I).

(K) Quantification of the mobile and immobile fractions as in (I). n = 10 cells.

(L) Quantification of GFP-LIS1 and -NDEL1 fluorescence recovery as in the AIS of DIV7/8 neurons. n = 10 cells.

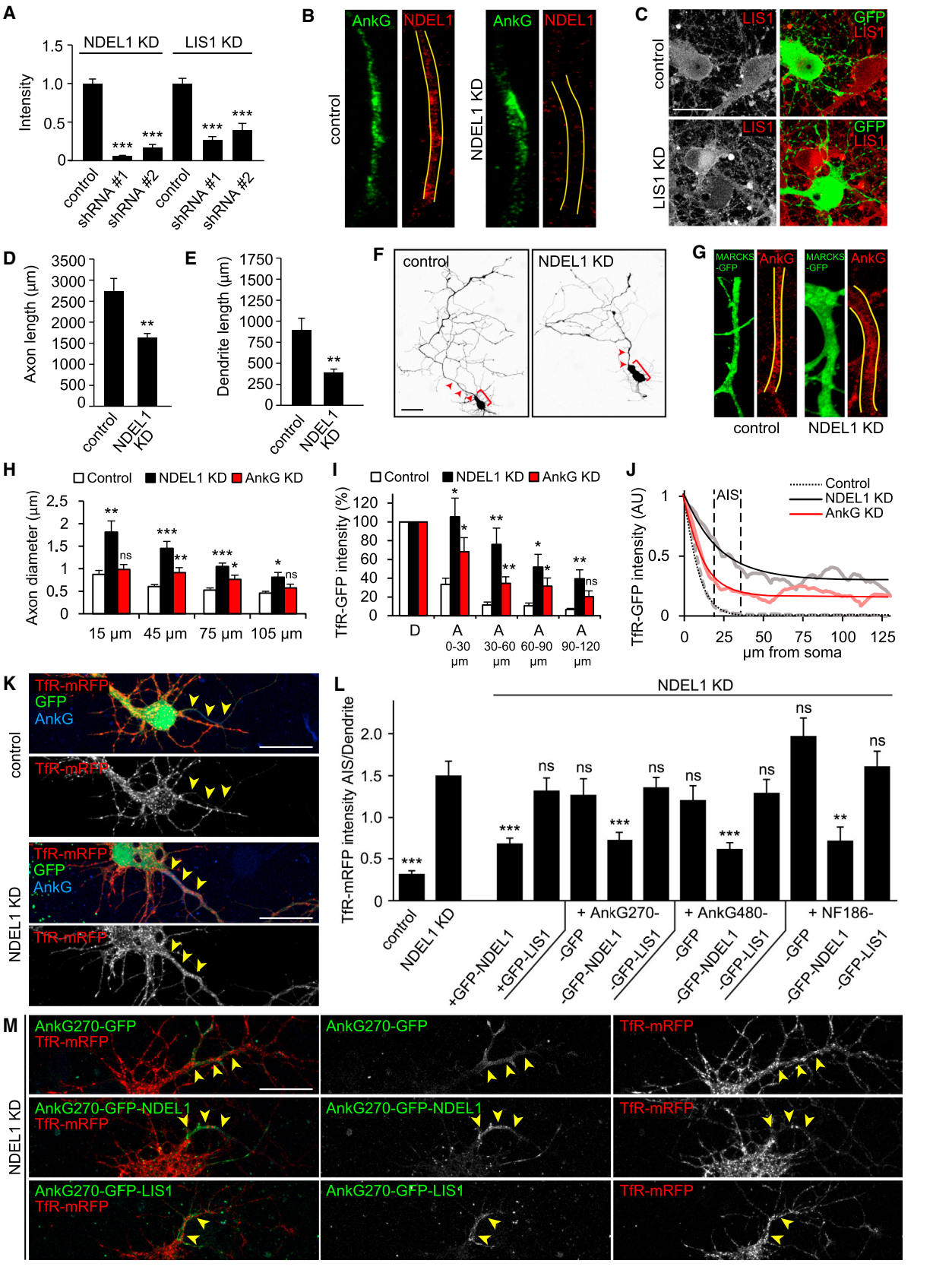

(legend on next page)

control neurons in the amount of dynamic MTs (Figure S6E), the direction of MT plus-end growth (Figure S6F) or the localization of non-centrosomal MT minus-ends (Figure S6G), the overall MT organization was disrupted. At sites of focal axonal swellings, MT bundles splayed and some MTs buckled (Figure S6H). Live imaging revealed that MTs in the proximal axon deformed in NDEL1 knockdown neurons (Figures S6I and S6J), and FRAP experiments confirmed that MTs at the AIS of NDEL1-depleted neurons were less stable (Figure S6K). These MT organization alterations may be explained by mechanical stress, as was for example reported after axonal stretch injury (Tang-Schomer et al., 2012). Recently, dynein was proposed to counteract forces resulting from retrograde actin flow. As a result, dynein inhibition caused "en-masse" displacement of MTs toward the cell body and compacted axons (Roossien et al., 2014). To test whether NDEL1 depletion resulted in similar translocations, we tracked the movement of photoactivated patches of MTs in the proximal axon. Indeed, MTs of NDEL1 knockdown neurons relocated toward the soma at a rate of 0.95 μm/hr, as opposed to the relatively static MTs of control neurons (Figure S6L). These data, paired with the decrease in axon length (Figure 3D), suggest that the axonal enlargement observed in NDEL1-depleted neurons may result from axonal compaction as a consequence of force imbalances.

AIS-Localized NDEL1 Is Required for the Polarized Distribution of Somatodendritic Cargo

Because of NDEL1's specific localization at the AIS and its ability to regulate dynein, we hypothesized that NDEL1 could be involved in cargo sorting at the AIS. We therefore first examined the polarized distribution of the transferrin receptor (TfR), a recycling transmembrane protein strictly localized to the somatodendritic region. In control cells, TfR-GFP was excluded from the axon starting at the AIS (Figures 3I–3L, S4E, and S4F). However, after depletion of NDEL1, TfR appeared in the axon (Figures 3I–3L, S4E, and SF) and in some cases accumulated at the AIS (Figure S7A). Consistently, the observed mistargeting of TfR was rescued by co-expressing NDEL1 or NDE1 but not LIS1 (Figure S7B). In these experiments, some neurons showed non-polarized TfR trafficking without axonal enlargement and vice versa (Figures S5G and S5H), suggesting that there is no causative relation between axonal enlargement and trafficking defects. In addition, TfR transport was non-selective upon both LIS1 depletion and dynein inhibition (Figures 4A–4C, S7C, and S7D). Together, these data demonstrate that NDEL1, LIS1, and dynein are required for the polarized distribution of TfR vesicles.

We also assessed the behavior of mitochondria and Rab3-positive synaptic vesicle precursors, as well as the distribution of the somatodendritic coxsackie and adenovirus receptor (CAR) and AMPA receptor subunits GluR1 and GluR2, and confirmed a more general role for NDEL1 in selective cargo trafficking (Figures S7E–S7O) consistent with previous studies. Finally, to test the importance of NDEL1's localization at the AIS, we examined TfR trafficking in AnkG-depleted neurons. Albeit less efficiently than in NDEL1 knockdown neurons, we found that TfR vesicles entered the axon (Figures 3I and 3J). Additionally, we displaced endogenous NDEL1 from the AIS by overexpressing the NDEL1 C terminus. In neurons overexpressing NDEL1-C, TfR vesicles moderately entered the AIS, while axons did not enlarge (Figures S5I and S5J). In addition, we fused full-length NDEL1 to AIS-immobilized proteins and used these chimeric proteins to rescue polarized TfR trafficking in the absence of endogenous NDEL1. We found that both fusions of NDEL1 to AnkG or neurofascin-186 (NF-186), a transmembrane AIS protein, prevented axonal entry of TfR (Figures 3L and 3M). By contrast, AIS-targeted fusions of LIS1 or GFP to NF-186 or AnkG were not able to rescue this phenotype (Figures 3L and 3M). Our data suggest that NDEL1 localization to the AIS contributes to efficient local somatodendritic cargo reversal.

NDEL1 Reverses the Direction of Somatodendritic Vesicles at the AIS

We next tested how NDEL1 depletion affects axonal and dendritic vesicle transport dynamics at the AIS using live cell imaging. In control neurons, TfR vesicles that entered the axon paused (~34%), reversed direction (~55%), or proceeded through the AIS (~11%) (Figures 4E–4G). In NDEL1 knockdown neurons, ~50% of TfR vesicles paused, while only ~5% reversed direction and ~45% of vesicles proceeded through the AIS into more distal parts of the axon (Figures 4F and 4G). By contrast, TfR movement in dendrites was unaffected

Figure 3. NDEL1 Is Required for Axon Morphology and Polarized Cargo Trafficking

(A) Quantification of NDEL1 and LIS1 levels at the AIS (NDEL1) or soma (LIS1) of knockdown (KD) neurons.

(B) AISs of DIV7 neurons co-expressing βgal (data not shown) and control (empty pSuper) or NDEL1-shRNA, stained for NDEL1 (red) and AnkG (green).

(C) Neurons transfected with GFP and control or LIS1 shRNA, stained for LIS1 (red).

(D and E) Quantification of total axon (D) and dendrite length (E) in control and NDEL1 knockdown neurons. n = 8–20 cells.

(F and G) DIV7 neurons transfected with control or NDEL1-shRNAs and β-gal (F) or MARCKS-GFP (G) to visualize morphology. (F) Red arrows indicate the AIS, brackets indicate the soma. (G) AnkG staining (red) indicates the AIS.

(H) Quantification of axon diameter of DIV8 neurons co-transfected with β-gal and indicated constructs, measured at the indicated distances from the soma. n = 10 cells.

(I) Quantification of TfR-GFP fluorescence intensity in neurons as described for (H), measured as the average intensity of various axonal segments (A, indicated distances) and normalized to dendrites (D). n = 10 cells.

(J) Smoothened TfR-GFP fluorescence intensity plots along axons of a single representative control, NDEL1 KD and AnkG KD neuron as described in (H). Values were normalized to the highest in the dataset.

(K) DIV7 control neurons (top) or NDEL1 depleted neurons (bottom) co-transfected with TfR-mRFP and GFP (fill), and stained for AnkG (blue). Yellow arrowheads indicate the AIS.

(L) Quantification of the ratio of TfR-mRFP fluorescence intensity (AIS/dendrites) of neurons in the specified conditions. n = 15–20 cells.

(M) DIV7 neurons depleted of NDEL1 and co-transfected with TfR-mRFP and indicated AnkG270-GFP-fusions.

Data are presented as means ± SEM, *p < 0.05, **p < 0.01, ***p < 0.001. Scale bars represent 20 μm in (C), 50 μm in (F), and 30 μm in (K) and (M).

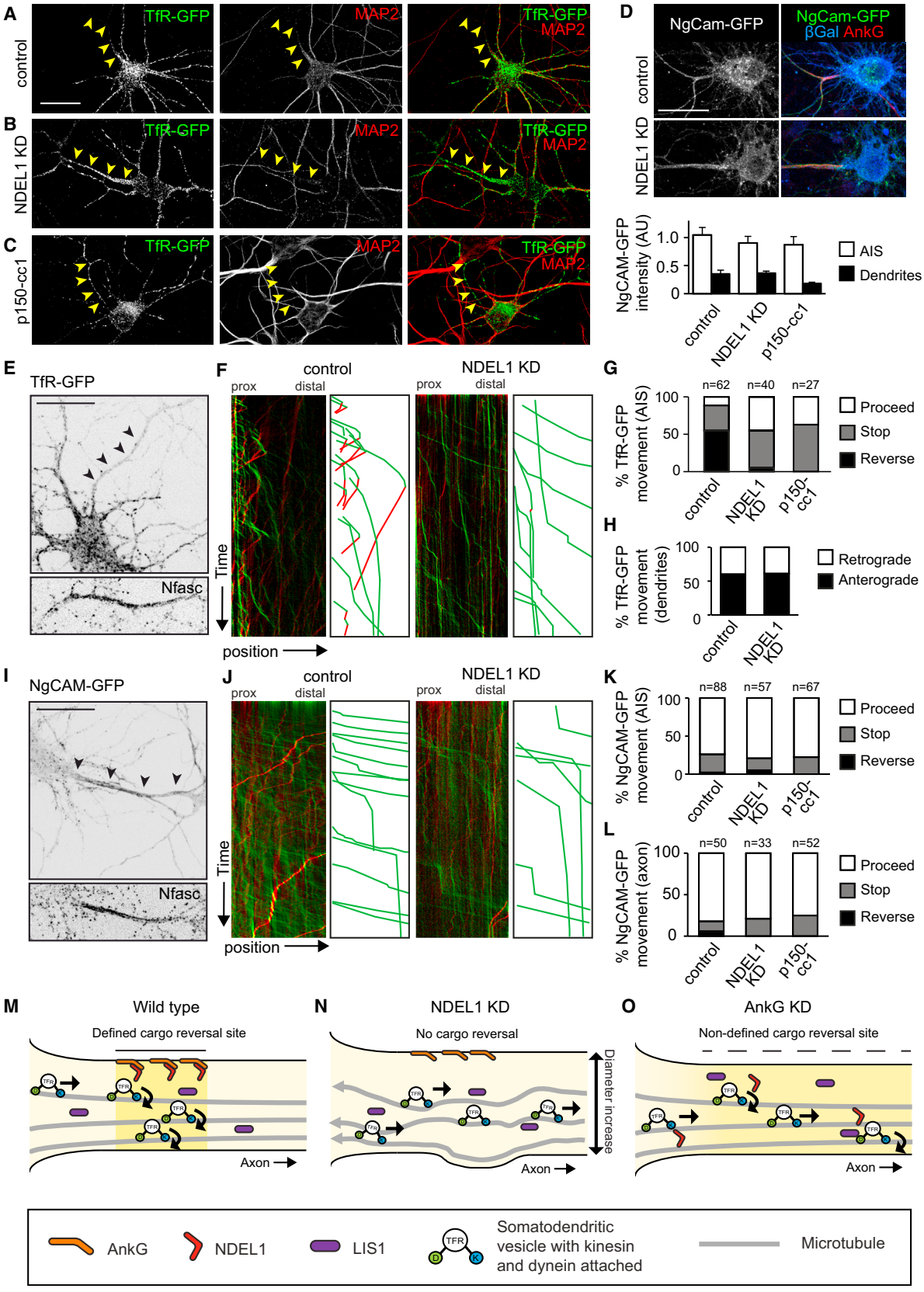

(legend on next page)

(Figure 4H). Similar results were obtained by overexpression of p150-cc1 (Figure 4G). Importantly, transport of axonal vesicles labeled by NgCAM-GFP was not affected by NDEL1 knockdown and p150-cc1 expression (Figures 4D and 4I–4L). Together, these results show that dynein and NDEL1 reverse the direction of somatodendritic vesicles.

Dynein Drives Retrograde Transport at the Proximal Axon

Previous work suggested a role for Myosin motors in the retrograde transport of cargo at the AIS (Al-Bassam et al., 2012; Lewis et al., 2009; Watanabe et al., 2012). To compare the transport capacity of dynein and myosin at the AIS, we used an inducible cargo trafficking assay in which we trigger the binding of specific motor proteins to peroxisomes during live-cell recordings (Kapitein et al., 2010, 2013) (Figure S8A). Coupling of dynein to peroxisomes via BICDN markedly increased the number of peroxisomes moving out of the AIS toward the soma (Figures S8B–S8D), consistent with dynein-mediated retrograde transport toward MT minus-ends in axons. However, very little cargo motility was observed upon recruitment of Myosin motors (Figures S8B–S8D), indicating that Myosin-V/VI is able to halt but not displace cargos in the proximal axon. These results support the view that dynein can drive retrograde cargo movement and that NDEL1 may serve as a positive regulator of dynein activity at the AIS.

DISCUSSION

AnkG Anchoring of NDEL1 Filters Intracellular Transport at the AIS

The AIS is believed to be involved in the regulation of axon-dendrite polarity by controlling intracellular transport (Leterrier and Dargent, 2014). Here we show that NDEL1 specifically localizes to the proximal axon via its C-terminal interaction with AnkG. The highly conserved N terminus of NDEL1 binds to LIS1 and is critical for dynein activity (Derewenda et al., 2007; Wang and Zheng, 2011), providing a direct link between a core AIS scaffold and dynein regulation. NDEL1 is stably present at the AIS and may transiently activate dynein on cargos that enter the proximal axon. An accumulation of regulatory proteins at the AIS might efficiently control intracellular transport, by making it possible to precisely modulate the activity of dynein-attached cargos during axonal entry. We speculate that NDEL1 is a limiting factor for dynein activity in the proximal axon and that high local concentration of NDEL1 facilitates rapid activation of dynein motors. This allows for quick switches of transport direction in a precisely defined axonal region (Figure 4M). Accordingly, loss of NDEL1 causes somatodendritic cargo to be retained at the AIS or to proceed into the axon (Figure 4N). NDEL1 redistribution caused by loss of AnkG results in moderate entry of somatodendritic cargo into axons, most likely because cargo reversals are not prevented by loss of dynein function but now occur in a larger, less-defined axonal region (Figure 4O). Thus, the link between AnkG and NDEL1 has important implications for filtering intracellular transport through the AIS.

Model for Controlling NDEL1-Mediated Dynein Activity at the AIS

Several observations have suggested that transport vesicles maintain a stable population of distinct motors. In such a model, regulatory proteins such as NDEL1 modulate the activities of specific motors present on cargo. We envision that kinesin motors driving dendritic vesicles into the axon are halted at the AIS, possibly by myosin motors. When dynein is locally activated, the cargo moves toward the MT minus-end back to the soma. Consistent with this model, NDEL1 has been shown to act as an upstream dynein regulator to enhance efficient minus-end-directed transport (McKenney et al., 2010; Niethammer et al., 2000; Sasaki et al., 2000). However, it remains unclear how AnkG-anchored NDEL1 activates dynein on dendritic cargo vesicles, either by directly contacting vesicles during axonal entry or by transiently recruiting regulatory factors that modulate dynein activity. In both scenarios, LIS1 is likely an important co-regulator of dynein activity at the AIS. Since LIS1 interacts with both NDEL1 and dynein (Niethammer et al., 2000; Sasaki et al., 2000) and is enriched but not stably bound to the AIS, we suggest a model in which cytoplasmic LIS1 shuttles between AnkG-NDEL1 at the membrane and dynein on dendritic cargo vesicles. In this scenario, NDEL1 may activate LIS1 molecules by conformational rearrangement or other regulatory mechanisms. Given the fast exchange of LIS1 at the AIS, this creates a pool of activated LIS1 molecules that may intercept dynein on dendritic cargo vesicles and subsequently promote dynein motor activity. This model also implies that dynein motors bound to dendritic vesicles are particularly sensitive to specific co-factors, which may be part of a general mechanism to assign individual dyneins for specific modes of cargo regulation (Vallee

Figure 4. NDEL1 Affects Somatodendritic Vesicle Behavior at the AIS

(A–C) DIV10 neurons co-transfected with TfR-GFP and indicated constructs and stained for MAP2 (red).

(D) Images (top) and quantification of NgCAM-GFP fluorescence intensity (bottom) at the AIS and dendrites of DIV8 neurons, transfected with indicated constructs and stained for AnkG (red).

(E and F) Kymographs illustrating the behavior of TfR-GFP vesicles at the AIS of live DIV7 neurons, co-transfected with TfR-GFP and control (E and F) or NDEL1-shRNA (F). AIS is highlighted by neurofascin (Nfasc) staining. Anterograde traces are in green, retrograde traces are red.

(G and H) Quantification of TfR vesicle dynamics at the AIS (G) and dendrites (H) of neurons as described for (E) and (F), as well as DIV7 neurons co-transfected with TfR-GFP and HA-p150-cc1 (G). The number of events is shown above the graph.

(I–L) Live cell imaging analysis of the behavior of NgCAM-GFP vesicles in control, NDEL1 KD and HA-p150-cc1 overexpressing neurons as described for (E)–(H).

(I) DIV7 neuron co-transfected with NgCAM-GFP and control vector. Kymographs show the behavior of NgCAM-GFP vesicles in control and NDEL1 knockdown neurons (J). Quantification of axonal vesicle dynamics inside the AIS is shown in (K). The behavior of vesicles exiting the AIS into the axon is quantified up until leaving the field of view in (L).

(M–O) Schematic depiction of somatodendritic vesicle behavior and microtubule architecture in control (M), NDEL1 KD (N), and AnkG KD neurons (O).

Scale bars represent 30 μm in (A) and (D), and 20 μm in (E) and (I). Data are presented as means ± SEM, *$p < 0.05$, **$p < 0.01$, ***$p < 0.001$.

et al., 2012). Future studies are required to systematically test the combined regulatory actions of NDEL1 and LIS1 on cargo-specific dynein.

EXPERIMENTAL PROCEDURES

See all information in Supplemental Experimental Procedures.

SUPPLEMENTAL INFORMATION

Supplemental Information includes Supplemental Experimental Procedures and eight figures and can be found with this article online at http://dx.doi.org/10.1016/j.neuron.2016.01.022.

AUTHOR CONTRIBUTIONS

M.K. and D.v.d.W. designed and performed biochemical and imaging experiments and wrote the manuscript, A.F. performed CRISPR-Cas9 experiments, A.C. performed live imaging and dSTORM experiments, R.J.C.R. and J.H. cloned shRNA constructs and performed antibody staining experiments; M.A.F. performed the rapalog-inducible cargo trafficking assay; L.C.K. and A.A. gave advice throughout the project; D.J. performed the immunohistochemistry on brain sections; C.C.H. supervised the research, coordinated the study, and wrote the manuscript.

ACKNOWLEDGMENTS

We thank Dr. Arai for the NDEL1 and NDE1 antibodies and Dr. J. Demmers and Ing. K. Bezstarosti for help with mass spectrometry analyses. This work was supported by Netherlands Organization for Scientific Research (NWO-ALW-VICI), the Netherlands Organization for Health Research and Development (ZonMW-TOP), and the European Science Foundation (EURYI). The authors declare no competing financial interests.

Received: September 22, 2014
Revised: June 15, 2015
Accepted: December 8, 2015
Published: February 3, 2016

REFERENCES

Al-Bassam, S., Xu, M., Wandless, T.J., and Arnold, D.B. (2012). Differential trafficking of transport vesicles contributes to the localization of dendritic proteins. Cell Rep. *2*, 89–100.

Derewenda, U., Tarricone, C., Choi, W.C., Cooper, D.R., Lukasik, S., Perrina, F., Tripathy, A., Kim, M.H., Cafiso, D.S., Musacchio, A., and Derewenda, Z.S. (2007). The structure of the coiled-coil domain of Ndel1 and the basis of its interaction with Lis1, the causal protein of Miller-Dieker lissencephaly. Structure *15*, 1467–1481.

Feng, Y., Olson, E.C., Stukenberg, P.T., Flanagan, L.A., Kirschner, M.W., and Walsh, C.A. (2000). LIS1 regulates CNS lamination by interacting with mNudE, a central component of the centrosome. Neuron *28*, 665–679.

Hedstrom, K.L., Ogawa, Y., and Rasband, M.N. (2008). AnkyrinG is required for maintenance of the axon initial segment and neuronal polarity. J. Cell Biol. *183*, 635–640.

Hippenmeyer, S., Youn, Y.H., Moon, H.M., Miyamichi, K., Zong, H., Wynshaw-Boris, A., and Luo, L. (2010). Genetic mosaic dissection of Lis1 and Ndel1 in neuronal migration. Neuron *68*, 695–709.

Incontro, S., Asensio, C.S., Edwards, R.H., and Nicoll, R.A. (2014). Efficient, complete deletion of synaptic proteins using CRISPR. Neuron *83*, 1051–1057.

Kapitein, L.C., and Hoogenraad, C.C. (2011). Which way to go? Cytoskeletal organization and polarized transport in neurons. Mol. Cell. Neurosci. *46*, 9–20.

Kapitein, L.C., Schlager, M.A., Kuijpers, M., Wulf, P.S., van Spronsen, M., MacKintosh, F.C., and Hoogenraad, C.C. (2010). Mixed microtubules steer dynein-driven cargo transport into dendrites. Curr. Biol. *20*, 290–299.

Kapitein, L.C., van Bergeijk, P., Lipka, J., Keijzer, N., Wulf, P.S., Katrukha, E.A., Akhmanova, A., and Hoogenraad, C.C. (2013). Myosin-V opposes microtubule-based cargo transport and drives directional motility on cortical actin. Curr. Biol. *23*, 828–834.

Leterrier, C., and Dargent, B. (2014). No Pasaran! Role of the axon initial segment in the regulation of protein transport and the maintenance of axonal identity. Semin. Cell Dev. Biol. *27*, 44–51.

Lewis, T.L., Jr., Mao, T., Svoboda, K., and Arnold, D.B. (2009). Myosin-dependent targeting of transmembrane proteins to neuronal dendrites. Nat. Neurosci. *12*, 568–576.

McKenney, R.J., Vershinin, M., Kunwar, A., Vallee, R.B., and Gross, S.P. (2010). LIS1 and NudE induce a persistent dynein force-producing state. Cell *141*, 304–314.

Nakata, T., and Hirokawa, N. (2003). Microtubules provide directional cues for polarized axonal transport through interaction with kinesin motor head. J. Cell Biol. *162*, 1045–1055.

Nguyen, M.D., Shu, T., Sanada, K., Larivière, R.C., Tseng, H.C., Park, S.K., Julien, J.P., and Tsai, L.H. (2004). A NUDEL-dependent mechanism of neurofilament assembly regulates the integrity of CNS neurons. Nat. Cell Biol. *6*, 595–608.

Niethammer, M., Smith, D.S., Ayala, R., Peng, J., Ko, J., Lee, M.S., Morabito, M., and Tsai, L.H. (2000). NUDEL is a novel Cdk5 substrate that associates with LIS1 and cytoplasmic dynein. Neuron *28*, 697–711.

Petersen, J.D., Kaech, S., and Banker, G. (2014). Selective microtubule-based transport of dendritic membrane proteins arises in concert with axon specification. J. Neurosci. *34*, 4135–4147.

Raaijmakers, J.A., Tanenbaum, M.E., and Medema, R.H. (2013). Systematic dissection of dynein regulators in mitosis. J. Cell Biol. *201*, 201–215.

Rasband, M.N. (2010). The axon initial segment and the maintenance of neuronal polarity. Nat. Rev. Neurosci. *11*, 552–562.

Roossien, D.H., Lamoureux, P., and Miller, K.E. (2014). Cytoplasmic dynein pushes the cytoskeletal meshwork forward during axonal elongation. J. Cell Sci. *127*, 3593–3602.

Sánchez-Ponce, D., Blázquez-Llorca, L., DeFelipe, J., Garrido, J.J., and Muñoz, A. (2012). Colocalization of α-actinin and synaptopodin in the pyramidal cell axon initial segment. Cereb. Cortex *22*, 1648–1661.

Sasaki, S., Shionoya, A., Ishida, M., Gambello, M.J., Yingling, J., Wynshaw-Boris, A., and Hirotsune, S. (2000). A LIS1/NUDEL/cytoplasmic dynein heavy chain complex in the developing and adult nervous system. Neuron *28*, 681–696.

Sasaki, S., Mori, D., Toyo-oka, K., Chen, A., Garrett-Beal, L., Muramatsu, M., Miyagawa, S., Hiraiwa, N., Yoshiki, A., Wynshaw-Boris, A., and Hirotsune, S. (2005). Complete loss of Ndel1 results in neuronal migration defects and early embryonic lethality. Mol. Cell. Biol. *25*, 7812–7827.

Segal, M., Soifer, I., Petzold, H., Howard, J., Elbaum, M., and Reiner, O. (2012). Ndel1-derived peptides modulate bidirectional transport of injected beads in the squid giant axon. Biol. Open *1*, 220–231.

Shu, T., Ayala, R., Nguyen, M.D., Xie, Z., Gleeson, J.G., and Tsai, L.H. (2004). Ndel1 operates in a common pathway with LIS1 and cytoplasmic dynein to regulate cortical neuronal positioning. Neuron *44*, 263–277.

Sobotzik, J.M., Sie, J.M., Politi, C., Del Turco, D., Bennett, V., Deller, T., and Schultz, C. (2009). AnkyrinG is required to maintain axo-dendritic polarity in vivo. Proc. Natl. Acad. Sci. USA *106*, 17564–17569.

Tang-Schomer, M.D., Johnson, V.E., Baas, P.W., Stewart, W., and Smith, D.H. (2012). Partial interruption of axonal transport due to microtubule breakage accounts for the formation of periodic varicosities after traumatic axonal injury. Exp. Neurol. *233*, 364–372.

Vallee, R.B., McKenney, R.J., and Ori-McKenney, K.M. (2012). Multiple modes of cytoplasmic dynein regulation. Nat. Cell Biol. *14*, 224–230.

Wang, S., and Zheng, Y. (2011). Identification of a novel dynein binding domain in nudel essential for spindle pole organization in Xenopus egg extract. J. Biol. Chem. *286*, 587–593.

Watanabe, K., Al-Bassam, S., Miyazaki, Y., Wandless, T.J., Webster, P., and Arnold, D.B. (2012). Networks of polarized actin filaments in the axon initial segment provide a mechanism for sorting axonal and dendritic proteins. Cell Rep. *2*, 1546–1553.

Youn, Y.H., Pramparo, T., Hirotsune, S., and Wynshaw-Boris, A. (2009). Distinct dose-dependent cortical neuronal migration and neurite extension defects in Lis1 and Ndel1 mutant mice. J. Neurosci. *29*, 15520–15530.

Zhang, X., and Bennett, V. (1998). Restriction of 480/270-kD ankyrin G to axon proximal segments requires multiple ankyrin G-specific domains. J. Cell Biol. *142*, 1571–1581.